Measurement of loss in superconducting microstrip at millimeter-wave frequencies

Jiansong Gao*, Anastasios Vayonakis*, Omid Noroozian*, Jonas Zmuidzinas*, Peter K. Day† and Henry G. Leduc†

*Division of Physics, Mathematics, and Astronomy, California Institute of Technology, Pasadena, CA 91125
†Jet Propulsion Lab, Pasadena, CA 91109

Abstract. We have developed a new technique for accurate measurement of the loss of superconducting microstrips at mm-wave frequencies. In this technique, we optically couple power to slot antenna, which is connected to one port of a hybrid coupler. One of the output ports of the hybrid delivers power to a series of mm-wave microstrip resonators which are capacitively coupled to a feedline followed by an MKID (microwave kinetic inductance detector) that measures the transmitted power. Two other MKIDs are connected to the remaining ports of the hybrid to measure the total incident optical power and the power reflected from the mm-wave resonators, allowing $|S_{21}|^2$ and $|S_{11}|^2$ to be accurately determined and resonance frequency f_r and quality factor Q to be retrieved. We have fabricated such a Nb/SiO_2/Nb microstrip loss test device which contains several mm- wave resonators with $f_r \sim 100$ GHz and measured it at 30 mK. All the resonators have shown internal quality factor Qi$\sim 500-2000$, suggesting a loss tangent of $\sim 5\times10^{-4}-2\times10^{-3}$ for the SiO_2 in use. For comparison, we have also fabricated a 5 GHz microstrip resonator on the same chip and measured it with a network analyzer. The loss tangent at 5 GHz derived from fitting the f_0 and Q data to the two-level system (TLS) model is 6×10^{-4}, about the same as from the mm-wave measurement. This suggests that the loss at both microwave and mm-wave frequencies is probably dominated by the TLS in SiO_2. Our results are of direct interest to mm/submm direct detection applications which use microstrip transmission lines (such as antenna-coupled MKIDs and transition-edge sensors), and other applications (such as on-chip filters). Our measurement technique is applicable up to approximately 1 THz and can be used to investigate a range of dielectrics.

Keywords: kinectic inductance detector, superconducting microstrip, loss tangent
PACS: 85.25.Oj

INTRODUCTION

Superconduting microstrips are useful in many mm/submm detection applications. For example, in a slot-antenna-coupled detection scheme, Nb microstrips are used in slot-antenna's summing network to coherently combine the radiation received from individual slots into a stronger signal, and to deliver the signal to the detectors, such as microwave kinetic inductance detectors (MKIDs)[1, 2, 3] and transition edge sensors (TESs)[4]. In addition, on-chip band-pass filters are often inserted between the antenna and the detector to define the receiving band (the color), which are also made from a microstrip structure[3, 5]. For all these applications, the microstrip loss at mm-wave frequencies is an important concern. Because the superconductor loss is usually small or negligible at frequencies below the gap frequency ($\sim$700 GHz for Nb), the microstrip loss is entirely dominated by the loss tangent δ of the dielectric layer in between the superconducting electrodes. This dielectric layer is often made of amorphous dielectric material (e. g., sputtered SiO_2). Therefore, accurate measurement of microstrip loss (or the loss tangent δ) at mm-wave frequencies becomes an important task. Previously, we have demonstrated a standing wave resonance technique to measure δ, in which superconducting tunnel junctions (STJs) are used to sense mm-wave power[6]. In this paper, we present another technique which is based on a microstrip resonator circuit and uses MKIDs to sense mm-wave power. This new technique is both accurate and easy to implement.

The design and principle of the microstrip loss test device, the measurement setup and our preliminary result will be presented in the subsequent sections of this paper.

MICROSTRIP LOSS TEST DEVICE

The design of the loss test device is illustrated (to scale) in Figure 1, which can be viewed as a circuit implementing a scalar 2-port measurement of mm-wave microstrip resonators. Mm-wave power is optically coupled into this circuit through a slot antenna (a, details on slot antenna can be found in reference [7]), which is connected to one port (port-1) of a hybrid coupler (b). One of the forward ports (port-2) of the hybrid delivers half of the total incident power $P_{\rm inc}/2$ to a series of mm-wave microstrip resonators (d) which are capacitively coupled to a microstrip feedline (c) followed by an MKID (e, MKID-1) that measures the transmitted power $P_{\rm tran}$. The other

CP1185, *Low Temperature Detectors LTD 13, Proceedings of the 13th International Workshop*
edited by B. Cabrera, A. Miller, and B. Young

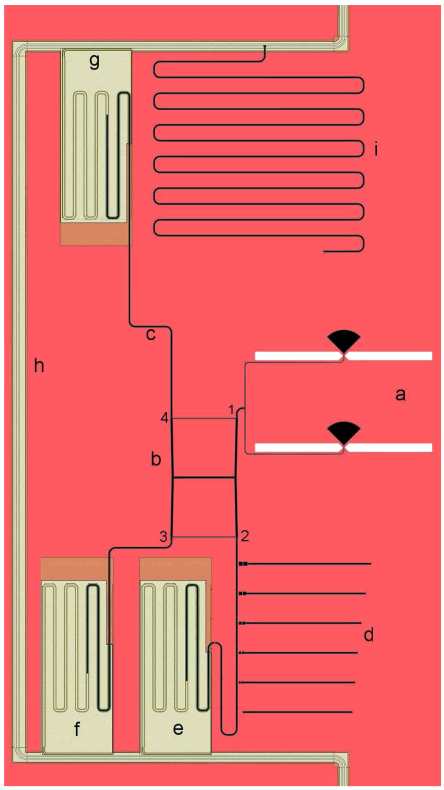

FIGURE 1. Design of the microstrip loss test device. a: Slot antenna. b: Hybrid coupler. c: Microstrip feedlines. d: Mm-wave microstrip resonators. e: MKID-1. f: MKID-2. g: MKID-3. h: CPW feedline. i: Microwave microstrip resonator.

forward port (port-3) of the hybrid is directly terminated by another MKID (f, MKID-2) which always sees $P_{\rm inc}/2$ and thus monitors the incident power. A third MKID (g, MKID-3) is connected to the reflection port (port-4) of the hybrid which measures the power $P_{\rm ref}$ reflected from the mm-wave resonators at port-2. All the 3 MKIDs are made of Al (both the center strip and the ground plane) and are read out through a common CPW feedline (h) that is also made of Al.

The transmission coefficient through the resonators and feedline is $|S_{21}|^2 = P_{\rm tran}/(P_{\rm inc}/2)$ which is given by the ratio of the signal measured by MKID-1 and MKID-2. Similarly, the reflection coefficient $|S_{11}|^2 = P_{\rm ref}/(P_{\rm inc}/2)$ is given by ratio of the signal measured by MKID-3 and MKID-2. If the mm-wave frequency ν is swept through the resonance frequencies f_r of the microstrip resonators, resonance peaks will be seen in the $|S_{21}(\nu)|$ curve and dips in the $|S_{11}(\nu)|$ curve. The quality factor Q and internal quality factor Q_i can be derived by fitting these two curves to the theoretical models [1]. The loss tangent δ can be inferred from the measured Q_i by $\delta = 1/Q_i$.

To make the measurement accurate, it is important for the mm-wave power on the feedline to be absorbed completely by the MKID without any reflection. This is achieved by running the Nb microstrip feedline on top of the center strip of Al CPW resonator of MKID for a sufficient length. This microstrip-to-CPW coupling scheme is identical to that used in the antenna-coupled MKIDs design and is discussed in more detail in[3].

We have also included a microwave frequency microstrip resonator (i, $f_r \sim 5$ GHz) on the same chip, to measure δ at microwave frequencies and to compare it with mm-wave measurement. This microstrip resonator is capacitively coupled to and measured through the same CPW feedline as used to read out the 3 MKIDs.

We have first fabricated a 100-GHz version of our loss test device. On a Si wafer we have patterned 6 mm-wave resonators with $f_r \sim$100-120 GHz, and one microwave resonator with $f_r \sim$5 GHz. Both the mm-mave and microwave resonators have the same microstrip geometry: the top strip is 7.5 μm wide, both the top strip and the ground plane are made from 600 nm-thick Nb films, and the dielectric layer is made of 400 nm-thick sputtered SiO_2. The CPW resonators (MKIDs) have a center strip width of 9 μm and gaps of 3 μm, and are made from a 40 nm thick Al film.

Measurement setup

The device is mounted in a dilution fridge which has a dewar window made of high-density polyethylene (HDPE). There are also two cold sapphire windows (no AR coating) and two metal mesh filters along the optical path. These windows and filters are transparent to the 100 GHz mm-wave but largely attenuate the radiation at shorter wavelengths. In addition, a hemi-spherical Si lens is glued to the substrate side of the device and centered in front of the slot antenna to fill its beam.

To generate the mm-wave, we use a W-band frequency tripler driven by a 0-40 GHz microwave synthesizer. The tripler is followed by a waveguide filter and a rectangular horn. With this mm-wave source, the output mm-wave covers the frequency range of $\sim 100-110$ GHz.

As the mm-wave frequency ν is swept, signal from the 3 MKIDs are recorded at each frequency either as frequency shifts ($\delta f_i,\ i = 1,2,3$) using a network analyzer (by fitting to the resonance curves of MKIDs) or as voltage signal ($\delta V_i,\ i = 1,2,3$) using an IQ mixer (see reference [8] for more details on MKID readout). In the latter case, the voltage signal from IQ mixer are measured using two lock-in amplifiers (for I and Q, $\delta V = \sqrt{\delta I^2 + \delta Q^2}$), with the mm-wave source amplitude-modulated at 1 KHz.

It can be shown from MKID theory[8] that

$$|S_{21}(\nu)| = \delta f_1/\delta f_2 = \delta V_1/\delta V_2 \qquad (1)$$

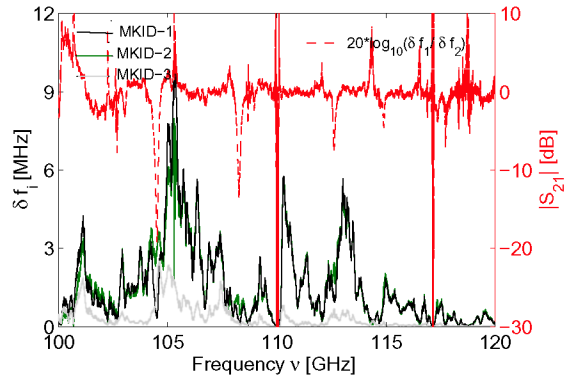

FIGURE 2. $|S_{21}(\nu)|$ derived from MKID frequency shifts measured using a network analyzer.

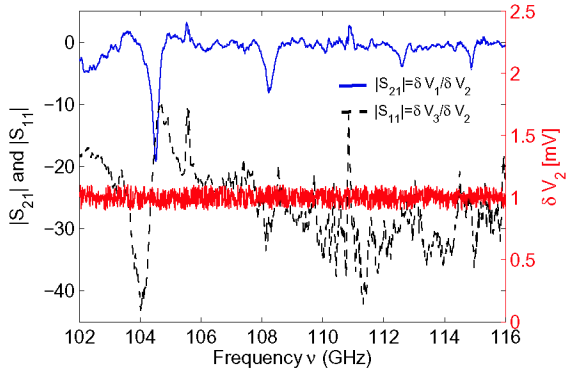

FIGURE 3. $|S_{21}(\nu)$ and $|S_{11}(\nu)|$ derived from MKID IQ voltage signal measured using lock-in technique.

$$|S_{11}(\nu)| = \delta f_3/\delta f_2 = \delta V_3/\delta V_2. \quad (2)$$

LOSS MEASUREMENT AT MM-WAVE FREQUENCY

Figure 2 shows the measured frequency shifts of the 3 MKIDs (left axis) and the derived $|S_{21}(\nu)|$ in a mm-wave frequency sweep from 100 GHz to 120 GHz. Four strong resonances clearly show up, with the resonance depths decreasing with frequency, which is consistent with the designed pattern of increasing Qc.

The sweep data shown in Figure 2 are taken with constant power driving the tripler. Because the gain of the tripler is highly frequency dependent, the output power varies strongly during the sweep, as can be seen from the oscillatory curve of δf_2. This is not desirable.

Figure 3 shows another sweep of $|S_{21}(\nu)|$ and $|S_{11}(\nu)|$ using the lock-in technique, with the output power of the tripler fixed instead. In this sweep, the power driving the

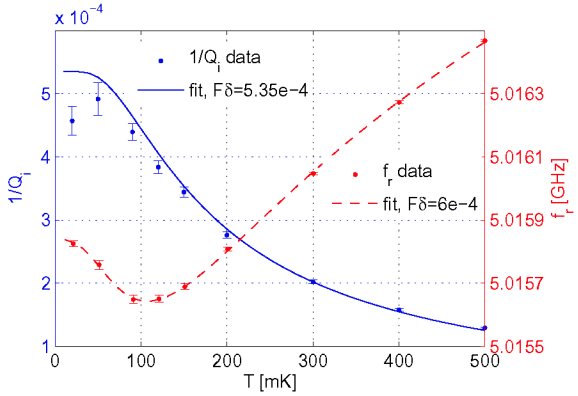

FIGURE 4. Temperature variation of Q_i and f_r measured from the microwave microstrip resonator. The solid and dashed lines show the fits to the TLS model. Both fits yield $F\delta \sim 6\times10^{-4}$, where $F \approx 1$ is the filling factor for the microstrip geometry. The $1/Q_i$ fit shows some deviation in the low temperature part, which is probably because the power used for the measurement is above the saturation power of the TLS at these temperatures.

tripler is adjusted at every frequency ν to keep the signal of MKID-2 fixed to $\delta V_2 \approx 1$ mV.

The $|s_{21}(\nu)|$ data in Figure 2 and Figure 3 are fitted to a Lorentzian model and the results are listed in Table 1 and Table 2, respectively. We find that fitting to both data sets yield the same resonance frequencies for the four resonators. Q_i varies from 1100 to 2200 in the first data set ($\delta = 5\times10^{-4} \sim 9\times10^{-4}$), and are slightly lower in the second data set, ranging from 500 to 1400 ($\delta = 7\times10^{-4} \sim 2\times10^{-3}$).

LOSS MEASUREMENT AT MICROWAVE FREQUENCY

The loss tangent δ at microwave frequency is measured from the 5 GHz microstrip resonator. Figure 4 plots the measured temperature variation of Q_i and f_r under low microwave power (internal power about -80 dBm), which shows the typical TLS behavior. Fitting to $1/Q_i(T)$ and $\delta f_r(T)$ data both yield a loss tangent of $\delta \sim 6\times10^{-4}$. The temperature sweep and TLS fitting technique used here is well described in reference [9, 10].

DISCUSSIONS

1. The microwave resonator data fits almost perfectly (especially the f_r data) to the TLS model, which suggests that the dominant loss mechanism at microwave

frequency is the TLS loss. We also find that δ measured at mm-wave frequency is not too different from that measured at microwave frequency. This implies that TLS loss is also dominating at mm-wave frequency, which is expected from the TLS theory [11, 12]. In fact, it is found that TLS has a very broad energy distribution and its density of states is almost flat across a wide frequency range, from MHz to THz.

2. The $|S_{21}|$ data measured from the two different approaches (shown in Figure 2 and 3) are actually also measured at different mm-wave power. From a calculation of MKID responsivity, we estimate the internal power in the mm-wave resonators to be $\sim 10 - -100$ nW for the network analyzer data (Figure 2) and ~ 4 pW for the lock-in data (Figure 3). The latter is close to the power level transmitted on the microstrip in the antenna-coupled MKIDs, so our low power measurement result is directly applicable there.

The derived δ shown in Table 1 and 2 only differ by about a factor of two, while the internal power varies by over 3 order of magnitude. It is very likely that within the range of mm-wave power we have probed, δ remains constant and instead, the apparent difference in Q_i, for different resonators and at different power, is probably due to the inaccuracy of our measurement (some possible causes for this inaccuracy are discussed later). Indeed, the TLS model predicts a δ that is both frequency and power independent as long as the power is lower than the saturation power and $kT \ll \hbar\omega$[13].

With these results, we are able to estimate the microstrip loss i antenna-coupled MKIDs, which is our initial motivation. In the antenna-coupled MKIDs design, the microstrip runs a total length of ~ 10 mm, including the feeding network of the antenna, the band-pass filter and the feedline to MKID[3]. If we take $\delta = 6 \times 10^{-4}$ at 300 GHz and a dielectric constant of 4 for SiO_2, the total loss in microstrip lines works out to be $\sim 8\%$, which is low enough for the application.

3. Our results presented in this paper is rather preliminary and we have run across a few problems in our measurement. As can be seen in both Figure 2 and Figure 3, the $|S_{21}|$ data are noisy; the on-resonance data is distorted from a Lorentian shape and the off-resonance data shows a lot of fringing and spikes. This leads to some difficulty in the resonator fitting and inaccuracy in the fitting result. We think the main reason for the poor data quality is because the optical configuration are not optimized. In the measurement, we shine the mm-wave source directly to the dewar window without an external lens and therefore the incident beam are not well matched to the antenna pattern. As a result, reflections and multi-path interference may be occurring. Also, the Al MKIDs can directly pick up the mm-wave radiation if the beam is too broad or poorly matched to the antenna. This might be part of the reason why resonance features are blurred or missing in the $|S_{11}|$ data. Another possibility is that the mm-wave power is not completely absorbed by the MKIDs at the end of the feedlines but is partially reflected back to the hybrid, which can certainly complicate both the $|S_{21}|$ and $|S_{11}|$ curves.

TABLE 1. Resonator fitting result for $|S_{21}|$ data in Figure 2

f_r **[GHz]**	Q	$\lvert S_{21}\rvert_{\min}$ **[dB]**	Q_i
104.66	242	19.1	2182
108.31	254	13.0	1135
112.57	671	7.0	1502
114.90	1250	4.3	2050

TABLE 2. Resonator fitting result for $|S_{21}|$ data in Figure 3

f_r **[GHz]**	Q	$\lvert S_{21}\rvert_{\min}$ **[dB]**	Q_i
104.67	156	19.1	1406
108.17	186	8.1	473
112.61	397	3.8	614
114.87	665	4.4	1103

With an improved design of the device and better optimization of the optical configuration, we think the data quality and the accuracy of our measurement can be significantly improved. Our measurement technique is applicable up to approximately 1 THz and can be used to investigate a range of dielectrics.

REFERENCES

1. P.K. Day, et al., *Nature* **425**, 817 (2003)
2. P. K. Day, et al., *Nucl. Instr. and Meth. in Phys. Res. A* **559**, 561–563 (2006).
3. J. Schlaerth, et al, *J. Low Temp. Phys.* **151**, 684–689 (2008).
4. C. L. Kuo, et al, *Proc. of the SPIE 7020*, 70201I (2008).
5. S. Kumar, *PhD Thesis*, Caltech, (2007).
6. Vayonakis A, et al, *AIP Conf. Proc. LTD-9*, 539–542 (2002).
7. J. Zmuidzinas, et al, *IEEE Tran. on Microwave Theory and Techniques* **40**, 1797–1804 (1992).
8. J. Gao, *PhD Thesis*, Caltech, (2008).
9. J. Gao, et al, *Appl. Phys. Lett.* **92**, 152505 (2008).
10. S. Kumar, et al., *Appl. Phys. Lett.* **92**, 123503 (2008)
11. W. A. Phillips, *J. Low Temp. Phys.* **7**, 351 (1972).
12. P. W. Anderson, et al., *Philos. Mag.* **25** 1 (1972).
13. W. A. Phillips, *Rep. Prog. Phys.* **50** 1657 (1987).